Available online at www.eccomasproceedia.org
Eccomas Proceedia COMPDYN (2021) 4353-4362

ECCOMAS
Proceedia

COMPDYN 2021
8th ECCOMAS Thematic Conference on
Computational Methods in Structural Dynamics and Earthquake Engineering
M. Papadrakakis, M. Fragiadakis (eds.)
Streamed from Athens, Greece, 28 - 30 June 2021

NUMERICAL STUDY ON THE DAMPING CHARACTERISTICS OF A SHOCK ABSORBER VALVE UTILIZING DIFFERENT VELOCITIES THROUGH CFD ANALYSIS

Yousif Badri[1], Thaer Syam[1], Sadok Sassi[1*], Mohammed Hussein[2], Jamil Renno[1], Saud Ghani[1]

[1]Department of Mechanical and Industrial Engineering, College of Engineering, Qatar University, Doha, Qatar

[2] Department of Civil and Architectural Engineering, College of Engineering, Qatar University, Doha, Qatar

[1*]Corresponding author

E-mail: [1]*yb1903174@.qu.edu.qa,* [1]*thaer@qu.edu.qa ,* [1*]*sadok.sassi@qu.edu.qa,* [2]*mhussein@qu.edu.qa,* [1]*jamil.renno@qu.edu.qa,* [1]*s.ghani@qu.edu.qa*

Abstract. *Shock absorbers or hydraulic dampers are power dissipating devices. The fluid flow inside the damper is governed by predefined passages. The damping effect is accomplished by the resistance of oil to flow through the restrictions. The impact of the viscosity and the velocity of the oil determines the fluid flow behaviour and hence, the resulting damping effect. The piston inside the damper has various orifices or piston valves that cause different flow losses. These losses are observed during the extension and compression strokes of the damper. In the compression and extension strokes, rebound and compression pressures are developed at the damper orifice. In this work, Computational Fluid Dynamics (CFD) analysis is carried out on a rear side two-wheeler automobile mono tube damper to investigate the variation of the damping properties using viscous oils. Averaged Navier-Stokes equations are solved by the SIMPLE method and the RNG k-ε is used to model turbulence. The piston contains eight orifices which separate the rebound and compression chambers of the damper. The numerical analysis used four values of velocity; 0.8, 1, 1.2, and 1.5 m/s. The viscous fluid model was SVI2.5, having viscosity value of 0.009 Pa.s. The damping coefficient values for rebound and compression sides were obtained based on their pressure values showed in the CFD contour plots. It was noticed that the increasing trend of damping coefficient is linearly for two velocity's intervals; (0.8-1) m/s and (1.2-1.5) m/s, and nonlinearly for velocity interval of (1-1.2) m/s.*

Keywords: Hydraulic damper, viscosity, CFD, damping characteristics, orifice, and pressure contours.

ISSN:2623-3347
Peer-review under responsibility of the organizing committee of COMPDYN 2021.
doi: 10.7712/120121.8791.18767

1 INTRODUCTION

A shock absorber, or viscous damper, is mainly functioning to dampen body/suspension motions, control tire force variation, and dissipate impact energy. Hydraulic oil is passed between two chambers via a system of pressure sensitive flow restrictions. The damping effect is accomplished by the resistance of oil to flow through the restrictions. Most vehicular shock absorbers are either twin-tube or mono-tube types with some variations on these themes as shown in Fig. 1. Twin tube shock absorber consists of two nested cylindrical tubes, an inner tube that is called the "working tube" or the "pressure tube", and an outer tube called the "reserve tube". At the bottom of the device on the inside is a compression valve or base valve. When the piston is forced up or down, hydraulic fluid moves between different chambers via small holes or "orifices" in the piston and via the valve. The fluid movement converts the "shock" energy into heat which must then be dissipated. The mono-tube shock, which is a gas-pressurized shock and also comes in a coil over format, consists of only one tube, the pressure tube, though it has two pistons. The two pistons separate the shock's fluid and gas components. Mono tube shocks are typically found in trucks, vans, or vehicles used for hauling or transportation or driven in areas where harsh road conditions are common. While twin tube is found in cars and smaller SUVs, twin-tube shocks have a second cylinder specifically for internal fluid (Shams et al. [1]).

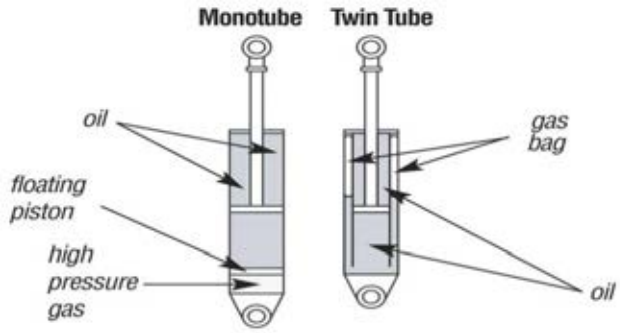

Fig. 1. Types of shock absorbers [1].

Generally, two main analytical models describe the viscous shock absorber behaviour; linear model, and generalized viscous damper model [2]. In linear model the damping force increases linearly as the velocity increases. On the other hand, generalized viscous model include the nonlinear behaviour of the damper force with respect to the change in velocity. The nonlinear behaviour provides a high damping force for the small vibration amplitudes (velocity). In viscous dampers, the linearity behaviour is governed by; orifice and damper geometry, fluid characteristics, and velocity of the vibrating structure. Many experimental studies were carried out to investigate the behaviour of fluid damper [3],[4]. For example, a recent experimental study conducted by Badri et al. [5] to investigate the effect of increasing velocity (increasing frequency) of mono tube damper in the damping coefficient value. In addition, numerical models are also used to characterize the viscous damper's damping effect. A physical model for a shock absorber was developed by Surace et al. [6]. This model provided a more realistic representation of the stiffness characteristics than previous simple models. Reybrouk et al. [7] presented a nonlinear physical model for predicting shock absorber performance. Dyum et al. [8] studied the mechanism of shock absorber rattling noise by valve behaviour analysis and CFD simulation. Herr et al. [9] identified valve parameters from several simple dynamometer tests and an additional incompressible model. These parameters

were then used to analytically determine valve flows for given pressure drops in the main model. Purdy et al. [10] evaluated the flow and performance of an automotive shock absorber by coupling a Computational Fluid Dynamics method with a dynamic modelling technique. They evaluated the pressure flow characteristics of the differing valve components using Computational Fluid Dynamics (CFD). Disk deformation information from finite element analysis simulations are incorporated into the calculation of blow-off valve opening. They obtained the damping force versus piston velocity curves. The radial flow of magnetic fluid under the piston of a magneto fluid shock absorber was studied by Tallec et al. [11]. Lee et al. [12] developed a non-linear model that includes the compressibility of the fluid, trapped gas and expansion of the cylinder. The performance of the shock absorber model was examined as the parameters were varied. Interaction of fluid and deformable structural parts in the shock absorber caused difficulties such as; compelling the kinematic compatibility at the fluid-structure interface and updating the geometry of the domain. Maikulal et al. [13] investigated the damping characteristics when the number of orifice holes changed using CFD. The numerical model results showed a nonlinear increase in the damping force with respect to the velocity increase.

In this paper, CFD simulations using ANSYS Fluent software is used to model a fluid flow inside the cylinder of a mono tube shock absorber. The damper's damping characteristics are investigated by changing the flow velocity using Rock Oil Rear shock fluid SVI2.5 oil as a viscous oil of the damper

This paper is outlined as follows; Section 1 introduces the topic and provides a literature review. Section 2 shows the methodology followed for the CFD starting from the governing equations and ending with the boundary conditions. Section 3 discusses the results and the main findings of this work. Finally, this paper ends at Section 4 which concludes and summarize the scope of this work as well as the main findings.

2 METHODOLOGY

This work will follow a methodology used by Maikulal et al. [13], when a CFD model simulates the flow inside a viscous damper. Following the same approach, a mono tube damper with new orifice design will be characterized over different velocities. The model is characterizing the viscous damper by calculating the damping coefficient at compression and rebound side based on their damping forces. Damping forces when using SIV-2.5 oil is analysed for different velocities and the variation of damping coefficient value will be investigated. In this section, the internal damper's chambers will be discussed, followed by the equations used to obtain the damping forces regarding constant velocities.

2.1 Damping characteristics of a damper

The scope of this work for the hydraulic damper is by identifying the damping action by allowing the hydraulic fluid (mainly a viscous fluid) to throttle through orifice in the piston (piston valve). The flow will be governed by the physical properties of the fluid such as viscosity and density, and the geometry of the piston valve (orifice). Mainly, the damper modelled for the CFD analysis is a piston cylinder system representing a mono tube shock absorber containing a hydraulic fluid as shown in Fig. 2 (a). The piston consists of; a rod and an orifice plate which connects two chambers (Chamber 1 and Chamber 2) showed in Fig. 2. The orifice plate has a small orifice which exposed to both piston sides and chambers of the

cylinder as shown in Fig. 2 (b). Chamber 1 represents the rebound piston side and chamber 2 represents the compression piston side.

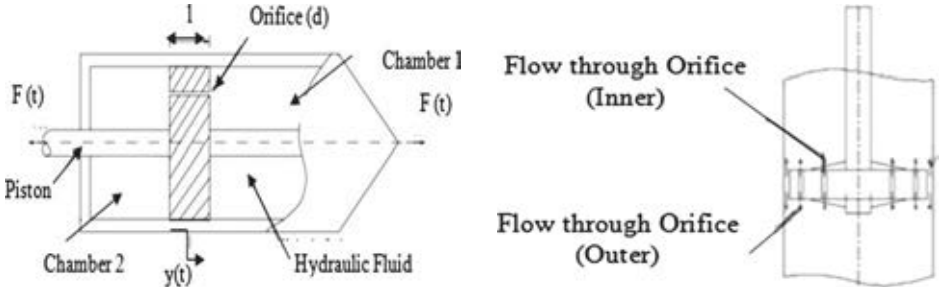

(a) (b)

Fig. 2. Hydraulic fluid flow through orifices [13].

The damping force is proportional to the velocity, as for a linear viscous damper, the damping force (F_d) may be related to the piston velocity (v) by Leea et al. [14]

$$F_d = c \times v \tag{1}$$

where F_d = damping Force (N), c = Damping Coefficient ($\mathrm{N.s/m}$), v = velocity of the piston (m/s).

The force of the piston in the two chambers is found by obtaining the pressure and the area on each piston side (compression and rebound). The force of the compression piston side is expressed by Guan et al. [15]

$$F_c = P_c \times A_c \tag{2}$$

$$F_r = P_r \times A_r \tag{3}$$

where $Fc\ and\ Fr$ are piston forces on compression and rebound side, respectively. Pc and Pr are the pressure on compression and rebound side (Pa), Ac and Ar are the area of piston on compression and rebound sides ($\mathrm{m^2}$).

3 NUMERICAL ANALYSIS

3.1 3D CAD modeling

In this study the orifice geometry was reproduced from dimensions used in Maikulal et al. [13]. The orifices plate was redesigned by modifying the number, and location of the orifice holes. 8 orifice holes are placed near the edge of the plate separated by an angle (45°). Top view of the orifice plate is shown in Fig. 3 (a). Fig. 3 (b) shows the 3D CAD drawing of the plate.

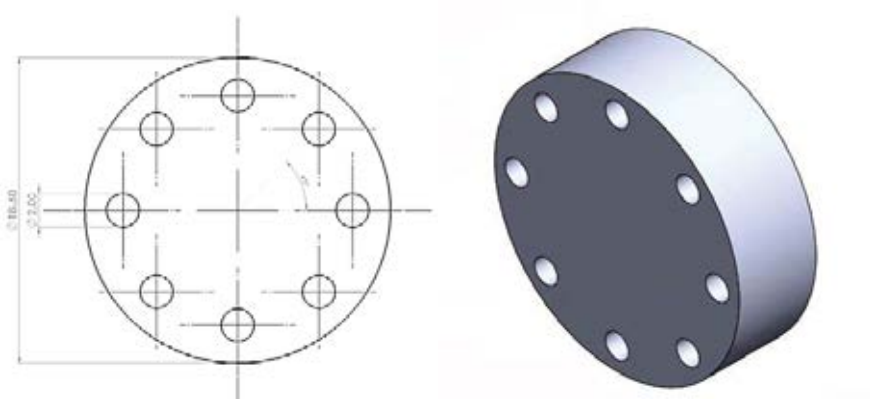

(a) (b)

Fig. 3. Orifice's geometry and orientation.

Fig. 4 shows the 3D drawing of the damper. The idea behind this model is that CFD simulation will be done inside the cylinder of the damper. This can be explained as the domain as shown in Fig. 4 (a); where the viscous oil will be moving through the orifice plate between the chambers at a specific velocity. Fig. 4 shows the 3D CAD model of the damper with 8 orifices in ANSYS.

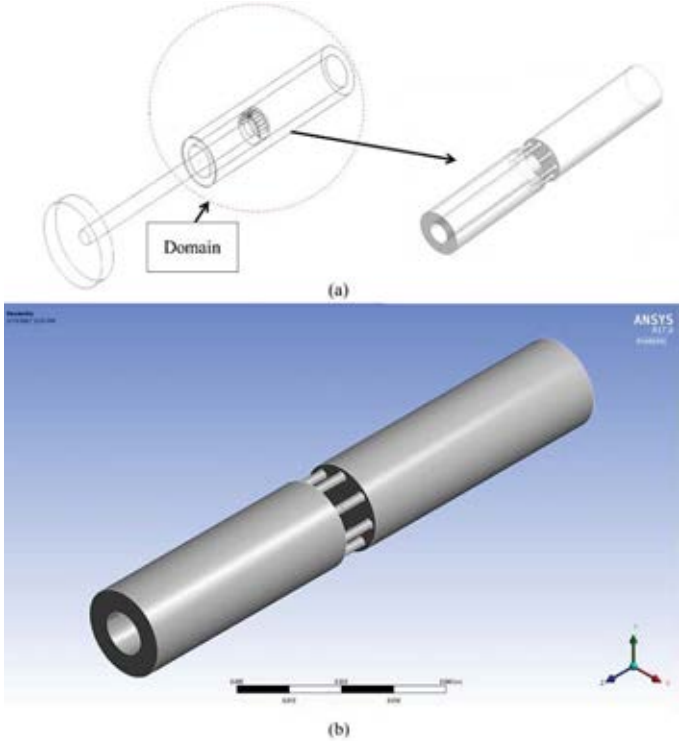

Fig. 4. 3D CAD drawings of the damper.

The CFD analysis will be based on throttling the viscous oil through the orifice of the three different cases. This will require the drawing of the inside domain of the cylinder. The oil will be throttled between the two chambers. Therefore, the domain will appear as a solid, but it will be considered as fluid in the CFD simulations. The orifice plate is placed at the midpoint of the length of the cylinder which is 118 mm. The volume of the orifice plate and the rod

(piston) is subtracted so that the domain is only fluid throttling through the orifice for the different three cases.

3.2. Mesh generation and quality

Unstructured automatic fine meshing with 3D tetrahedral cells was used. The meshing smoothing chooses to be high, while having a normal curvature angle of 15°. The mesh responded to high gradient and curvature areas by providing more cells to those areas. By increasing the number of cells at the throttling area, while having fewer elements at areas near the inlet, and the outlet ensure accurate results with less computational time. The grid is then generated having 445076 elements with 87552 nodes, as shown in Fig. 5.

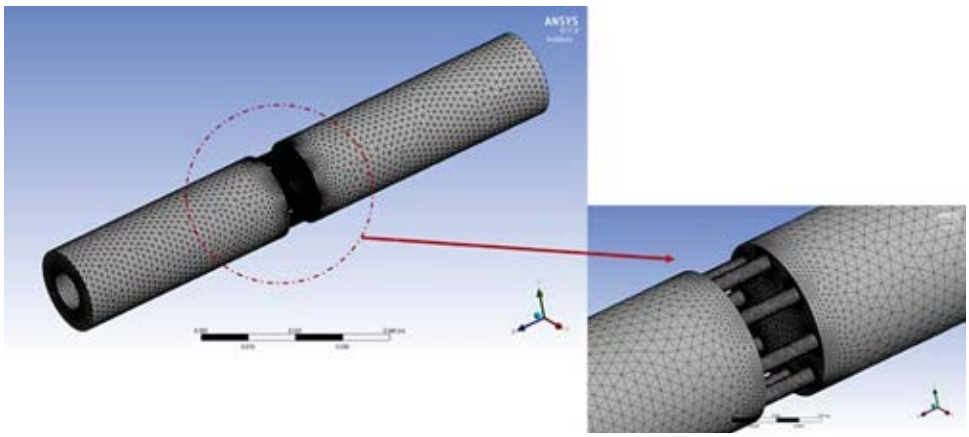

Fig. 5. Meshing.

3.3 CFD methodology, boundary conditions and simulation studies

The CFD modelling involves the numerical solution of the conservation equations in the laminar and turbulent fluid flow regimes. Therefore, the theoretical predictions were obtained by simultaneous solution of the continuity and the Reynolds averaged Navier-Stokes (RANS) equations. The governing equations for an incompressible flow are [16]

Conservation of mass:

$$\vec{\nabla}.(\vec{v}) = 0 \tag{4}$$

Conservation of momentum:

$$\rho\left[\frac{\partial(\vec{v})}{\partial t} + (\vec{v}.\vec{\nabla}.)\vec{v}\right] = \rho g - \nabla P + \mu\nabla^2\vec{v} \tag{5}$$

Since the flow in the shock absorber is in a state of turbulent motion, it is important to use an appropriate turbulence model for evaluating the flow field. The standard k–ε model is a semi-empirical model based on transport equations for the turbulent kinetic energy (k) and it is dissipation rate (ε). Improvements have been made to the model to improve its performance by the Realizable k–ε model [20]. Realizable k–ε model have shown substantial improvements over the standard k–ε model where the flow features include strong streamline curvature, vortices and rotation. The flow governing equations are solved with ANSYS FLUENT 17R. A standard wall functions is used in order for wall treatment since the most focus is on

the orifice plate. The velocity and pressure coupling used the SIMPLE algorithm with a second order upwind spatial discretization for a pressure-based study.

4. RESULTS AND DISCUSSION

Static pressure contours are required to identify the forces on the two orifice sides (rebound, compression). The pressure contours for the compression and rebound piston sides for one case are presented in Fig. 7 (velocity of 0.8 m/s and using SVI-25 oil; 0.009 Pa.s).

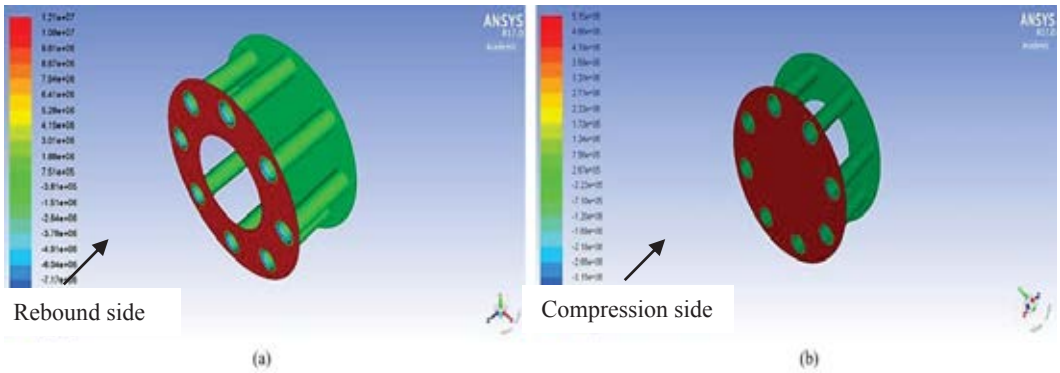

Fig. 6. Pressure contour for (a) rebound piston side, and (b) compression piston side.

The rebound-compression forces are calculated with respect to the maximum pressure value observed at the contour plot range. These forces are also related to the piston side surface areas. The compression side area is 1.8569 x10^{-4} m^2, and the rebound surface area is 2.4649 x10^{-4} m^2. The forces acting on small area (rebound) is greater than the forces acting on bigger area (compression) due to the pressure and area differences.

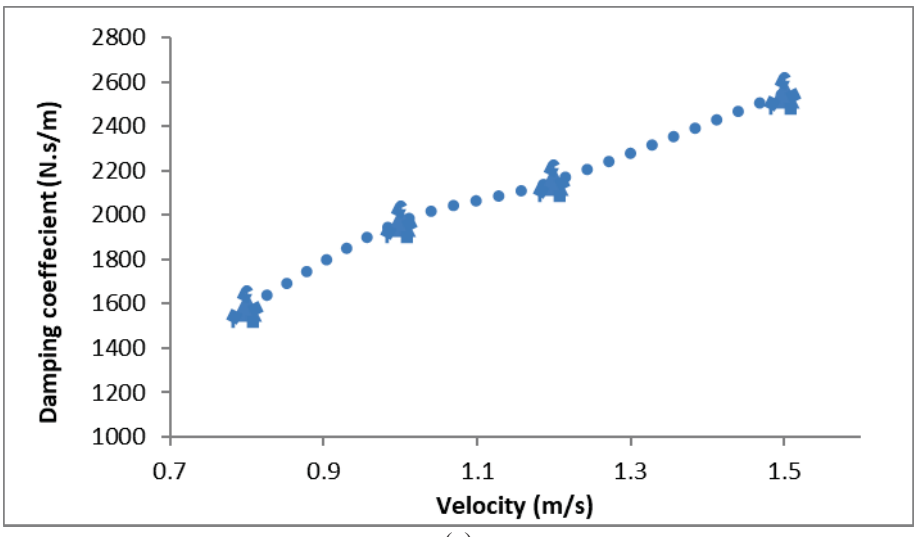

(a)

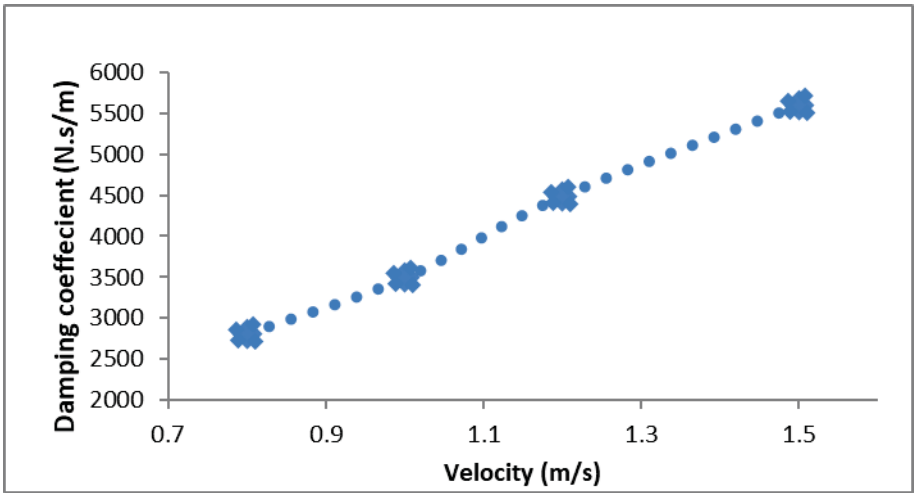

(b)

Fig. 7. Damping coefficient vs velocity (a) at the compression stroke (b) at the rebound stroke.

Damping values results are shown in Fig. 7 for the range of velocity of 0.8 m/s, 1 m/s, 1.2 m/s, and 1.5 m/s. Fig. 7 (a) shows the damping coefficient variation inside the compression chamber which was found to be; 1.59kN.s/m, 1.97kN.s/m, 2.15kN.s/m, 2.55kN.s/m, respectively. The damping coefficient inside the rebound chamber is shown in Fig. 7(b). The damping constant values with respect to the velocity range was found to be; 2.81kN.s/m, 3.5kN.s/m, 4.5kN.s/m, 5.6kN.s/m.

5 CONCLUSION

In this study, a CFD model was used to characterize a mono tube damper filled with SIV-2.5 oil over a range of velocity using Ansys 17 Fluent. The CFD model only takes into consideration the fluid chamber compressibility. However, the contribution of the internal friction in the damping force was omitted. Based on the obtained numerical damping coefficient values parametric the following was concluded:

1- Increasing the velocity tend to contribute in increasing the damping force, and hence the damping coefficient.

2- The damping values in both compression and rebound strokes are increasing linearly with the increase of velocity for two ranges; (0.8 - 1) m/s and (1.2 - 1.5) m/s. The damper is experiencing a nonlinear increase of the damping constant at the middle range of velocity of (1 - 1.3) m/s.

3- Using oil with low viscosity value (0.009 Pa.s) combines the linear-nonlinear behavior.

REFERENCES

[1] M. Shams and E. Reza (2007), “CFD-FEA analysis of hydraulic shock absorber valve behavior CFD-FEA ANALYSIS OF HYDRAULIC SHOCK ABSORBER VALVE,”.

[2] R. Greco and G. C. Marano, "A comparative study on parameter identification of fluid viscous dampers with different models," no. August, 2014.

[3] D. I. Narkhede and R. Sinha, "Behavior of nonlinear fluid viscous dampers for control of shock vibrations," *J. Sound Vib.*, vol. 333, no. 1, pp. 80–98, 2014.

[4] P. Torino, "Experimental determination of viscous damper parameters in low velocity ranges," no. July, 2017.

[5] Y. Badri, M. Hussein, S. Sassi, and J. Renno, "Investigation of the Effect of the Force-Frequency on the Behaviour of a New Viscous Damper for Railway Applications," no. Cic, pp. 666–671, 2020.

[6] Surace, C., Worden, K. and Tomlinson, G. R. (1992). An improved nonlinear model for an automotive shock absorber. *Nonlinear Dynamics* 3, 6, 413–429.

[7] Reybrouck, K. (1994). A nonlinear parametric model of an automotive shock absorber. *SAE Paper No.* 9400869.

[8] Morinaga, H., Kuboto, M. and Kume, H. (1997). Mechanism analysis of shock absorber rattling noise. *J. SAE Review* 18, 2, 198-198.

[9] Reybrouck, K. and Duym, S. (1998). A physical and parametric model for nonlinear dynamic and temperature dependant behaviour of automotive shock absorbers. *Proc. 11th ADAMS Users Conf.*, Frankfurt.

[10] Herr, F., Mallin, T., Lane, J. and Roth, S. (1999). A shock absorber model us ing CFD analysis and easy 5. *SAE Steering and Suspension Technology Symp.*, Detroit, Michigan, 267-281.

[11] Krakov, M. S. (1999). Influence of rheological properties of magnetic fluid on damping ability of magnetic fluid shock absorber. *J. Magnetism and Mag netic Materials,* 201, 368-371.

[12] Purdy, D. J. (2000). Theoretical and experimental investigation into an adjust able automotive damper. *Proc. Institution of Mechanical Engineers, Part D, J. Automobile Engineering* 214, 3, 265-283.

[13] L. Maikulal, S. Singh, and S. M. Sawant (2016), "Fluid flow modeling and experimental investigation on automobile damper," *Constr. Build. Mater.*, vol. 121, pp. 760–772.

[14] Choon-Tae Leea, Byung-Young Moonb (2004), Simulation and experimental validation of vehicle dynamic characteristics for displacement-sensitive shock absorber using fluid-flow modeling, Proceeding of Mechanical Systems and Signal Processing, vol. 20(2), Elsevier, pp. 373–388.

[15] Changbin Guan, Zongxia Jiao, Shouzhan He (2014), Theoretical study of flow ripple for an aviation axial-piston pump with damping holes in the valve plate, *J. Aeronaut*. 27 (1) 169–181.

[16] Gabriel J. DeSalvo and John A. Swanson. (1985). ANSYS engineering analysis system user's manual. Houston, Pa. :*Swanson Analysis* Systems,